Supporting Information

Protecting Li-metal anode with LiF-riched solid electrolyte interphase derived from fluorinated graphene additive

Xiaohong Wu[a*], Yuhao Hong[b], Zhengang Li[c], Junhao Wang[c], Haitang Zhang[c], Yu Qiao[c], Hongjun Yue[d*], Chunhai Jiang[a*]

[a] Fujian Provincial Key Laboratory of Functional Materials and Applications, Institute of Advanced Energy Materials, School of Materials Science and Engineering, Xiamen University of Technology, Xiamen, 361024, P. R. China

Email: xiaohongwu@xmut.edu.cn, chjiang@xmut.edu.cn

[b] Innovation Laboratory for Sciences and Technologies of Energy Materials of Fujian Province (IKKEM), Xiamen, 361024, P. R. China

[c] State Key Laboratory of Physical Chemistry of Solid Surfaces, College of Chemistry and Chemical Engineering, Xiamen University, Xiamen 361005, P. R. China

[d] CAS key Laboratory of Design and Assembly of Functional Nanostructures, and Fujian Provincial Key Laboratory of Nanomaterials, Fujian Institute of Research on the Structure of Matter, Chinese Academy of Sciences, Fuzhou 350002, P. R. China

Email: hjyue@fjirsm.ac.cn

Experimental Section

Materials Preparation: Base electrolyte with 1.0 M $LiPF_6$ in EC/EMC (3:7) was purchased from Suzhou Duoduo Chemical Technology Co., Ltd., China. F-Gr with 1 and 3 mg mL^{-1} were directly dissolved into base electrolyte. All electrolytes were stored in a glove box under Ar environment and utilized without further purification. The cathode slurries were prepared by mixing the cathode materials, conductive carbon and poly(vinylidene) fluoride (PVDF) with a mass ration of 8:1:1 in N-methyl-2-pyrolidone (NMP) solvent. The loading of active material on the cathode electrode is around 5 mg cm^{-2}.

Electrochemical measurements: In this work, all testing cells were used CR-2032 coin-type and assembled in Ar-filled glove box. The cyclic voltammetry (1.0 and 10.0 mV s^{-1}), linear sweep voltammetry (0.1 mV s^{-1}) measurement and electrochemical impedance spectroscopy (EIS) test were carried out on a CHI660E electrochemical workstation (Chenhua, China). A frequency range of 10^5 Hz to 10^{-2} Hz with an amplitude of 5 mV was applied for EIS test of cycled Li/Li symmetric cells. The galvanostatic cycling measurement were conducted on a Neware battery testing system (CT-4008T-5 V10 mA-164, Shenzhen, China) at room temperature. Before each charge/discharge measurement, the cells were kept on open circuit for 8~10 hours.

Characterizations: The Scanning Electron Microscopy (SEM) characterization was applied to observe the morphological difference of Li-metal anode between base and F-Gr contained electrolyte during continuous cycling in Li/Li symmetrical cells. It was conducted on Zeiss GeminiSEM 500 in the Tan Kah Kee Innovation Laboratory (Fujian Province), and corresponding images were obtained with an accelerating voltage of 1 kV. The tested cycled samples of Li-metal were rinsed by DMC to possibly wash off and remove the salt and residue solvent from the Li-metal surface, and evaporated in a vacuum chamber for around 30 min. Then samples can be

transferred to the SEM sample loading chamber via a vacuum transfer cassette. The X-ray photoelectron spectroscopy (XPS) characterizations was performed on the Thermo Fisher Scientific K-Alpha spectrometer for surface analyzations of cycled Li-metal. Depth profiling was realized by using Ar^+ sputtering. All XPS spectra were calibrated with the reference C-C peak at binding energy for 284.5 eV. Time-of-Flight secondary ion mass spectrometry (TOF-SIMS) measurement was conducted in the Tan Kah Kee Innovation Laboratory to investigate the specific components/compositions on cycled Li-metal surface, which is equipped with a 30 keV Bi_3^+ primary ion gun and a 1 keV Cs sputter gun for negative ion mode. For 2D chemical mapping and 3D depth profiling, the sputtering and analysis areas were set as 500 X 500 μm^2 and 100 X 100 μm^2, respectively.

a

b

C   F
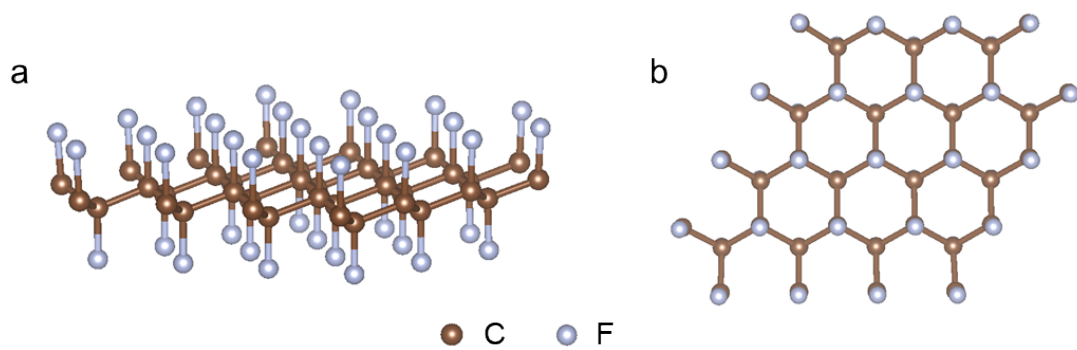
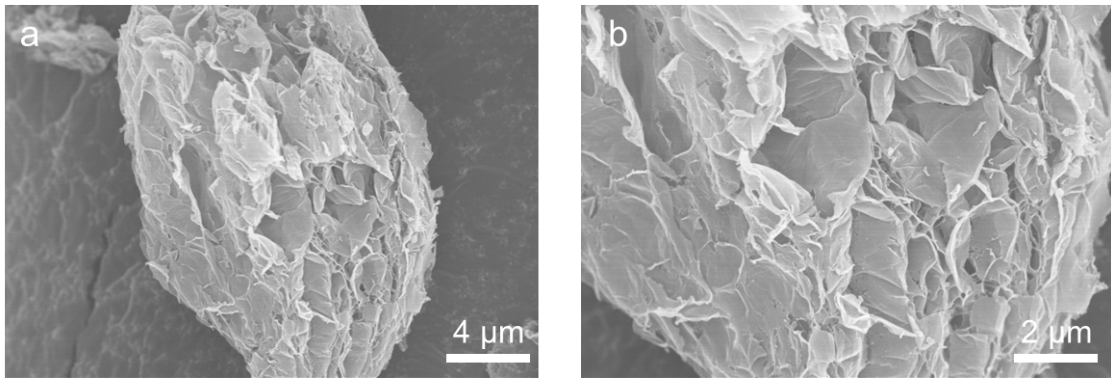**Figure S1.** The ball and stick models of the F-Gr by (a) front view and (b) side view.

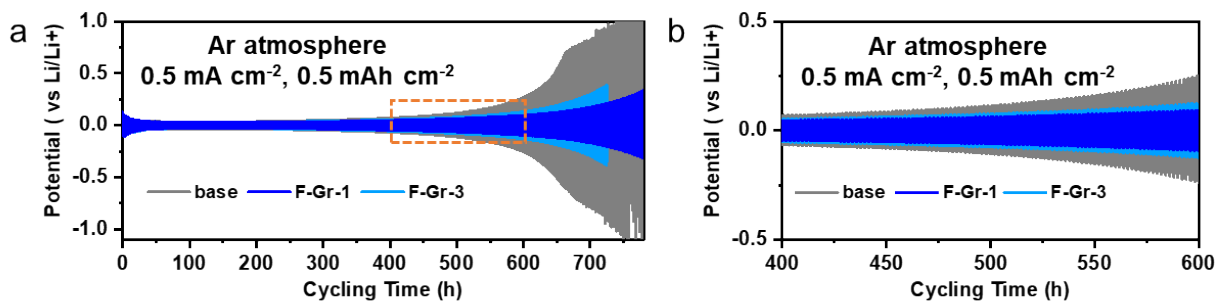**Figure S2.** SEM characterizations of F-Gr morphology at different magnifications.

Figure S3. Cycling stability of Li/Li symmetric cells with electrolyte containing different concentrations of F-Gr at a current density of 0.5 mA cm^{-2}.
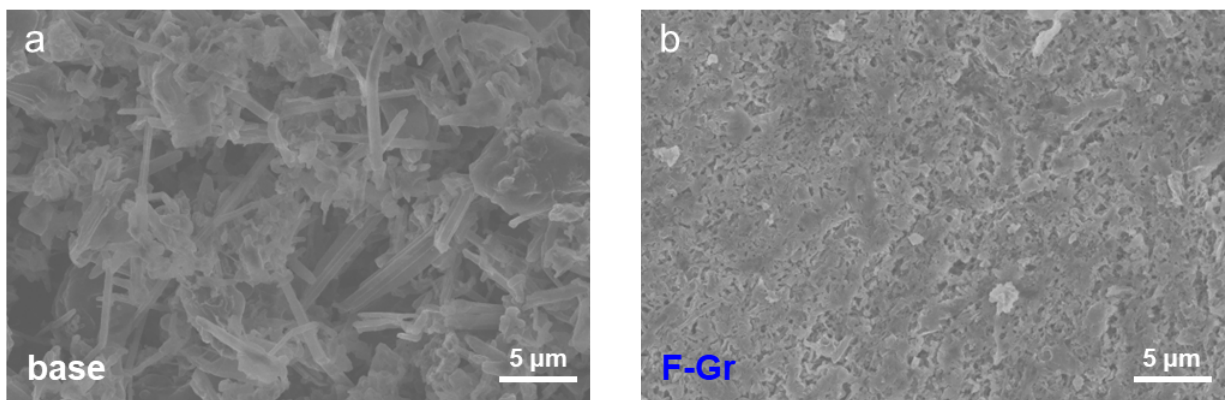
Figure S4. Magnified SEM images of cycled Li-metal in (a) base and (b) F-Gr-contained electrolytes after 50 cycles at 1.0 mA cm^{-2} with 1.0 mAh cm^{-2}.
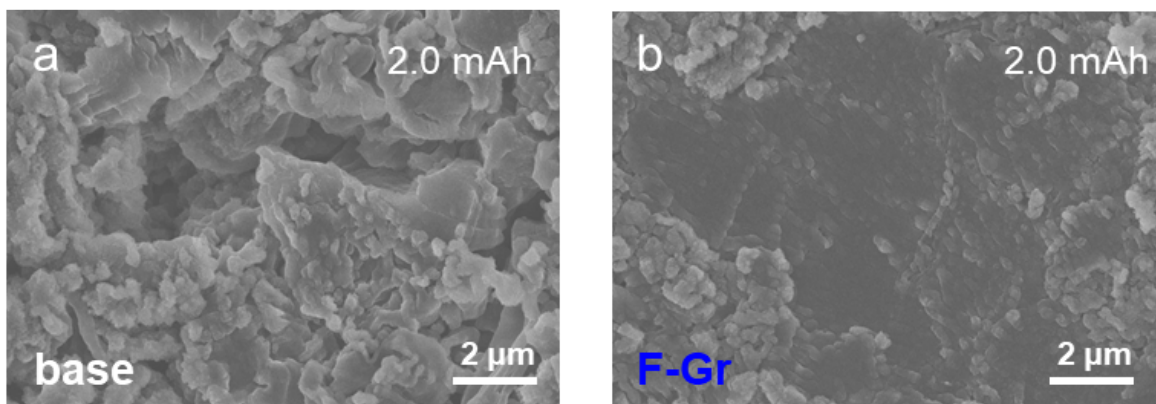
Figure S5. SEM images of Li deposition morphology on Cu substrate in LiPF$_6$-EC/EMC electrolyte (a) without and (b) with F-Gr (0.01 mA, 20 h).
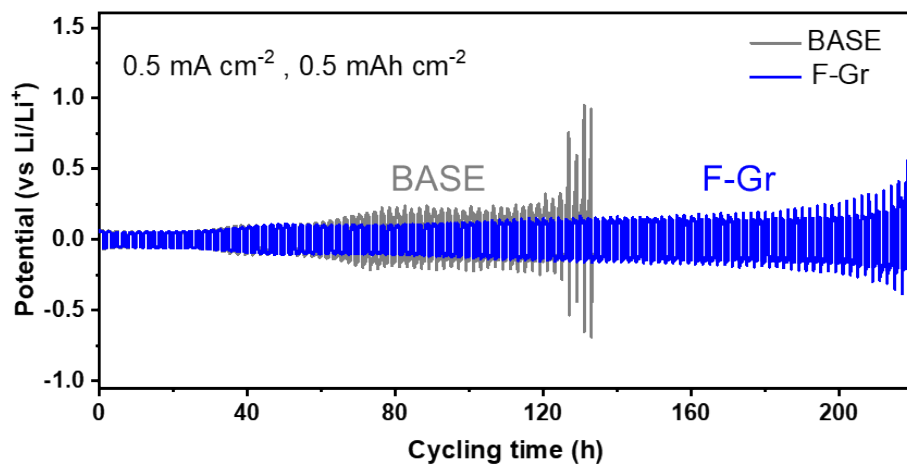
Figure S6. Cycling performance of Li/Li symmetric cells in ether-based electrolyte with/without F-Gr at a current density of 0.5 mA cm^{-2}.
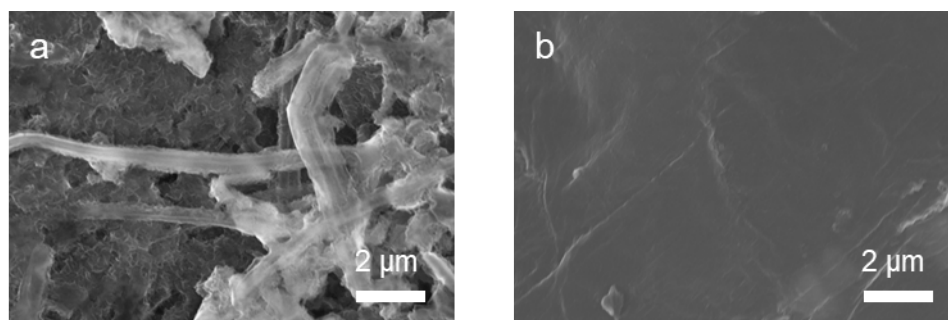
Figure S7. SEM images of cycled Li-metal in (a) BASE and (b) F-Gr-contained electrolytes after 50 cycles at 0.5 mA cm^{-2} with 0.5 mAh cm^{-2}.

Typical ether-based electrolyte, such as 1.0 M LiTFSI in TEGDME, is studied as "BASE electrolyte" to explore whether F-Gr can still protect Li-metal anode in ether-based electrolyte. Then Li/Li symmetrical cells are preferentially assembled to evaluate the effect of F-Gr on the cycling performance of batteries. As represented in Figure S6, longer lifespan and better cycling stability of Li/Li symmetrical cells can be realized in F-Gr-contained electrolyte than that in BASE (ether-based) electrolyte. After 50 cycles, significant dendrite growth can be observed on the Li-metal surface in BASE electrolyte as exhibited in Figure S7, which can accelerate the performance deterioration of Li/Li symmetrical cells (Figure S6, gray trace). However, Li-metal with relatively smooth and flat surface is well-preserved after 50 cycles in F-Gr-contained electrolyte, indicating that the introduction of F-Gr in ether-based electrolyte can effectively suppress detrimental dendrite growth and significantly enhance the cycling stability of Li/Li symmetrical cells. Therefore, not only ester-based electrolyte (1.0 M LiPF6 in EC/EMC in the manuscript) but also ether-based electrolyte (1.0 M LiTFSI in TEGDME), F-Gr can effectively suppress undesirable dendrite growth and improve the cycling performance of Li/Li symmetrical cells.
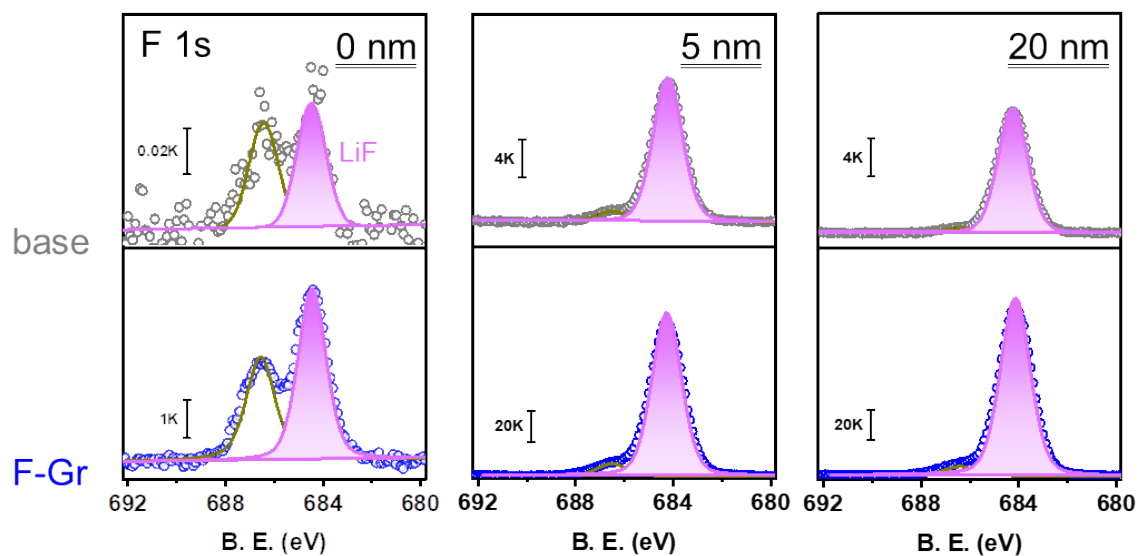
Figure S8. F 1s spectra for Li-metal cycled in base or F-Gr-contained electrolyte with a sputtering depth of 0, 5, 20 nm. The Li-metal is retrieved from Li/Li symmetrical cell after 50 cycles, which is cycled at 1.0 mA cm^{-2} with a fixed plating capacity of 1.0 mAh cm^{-2}.
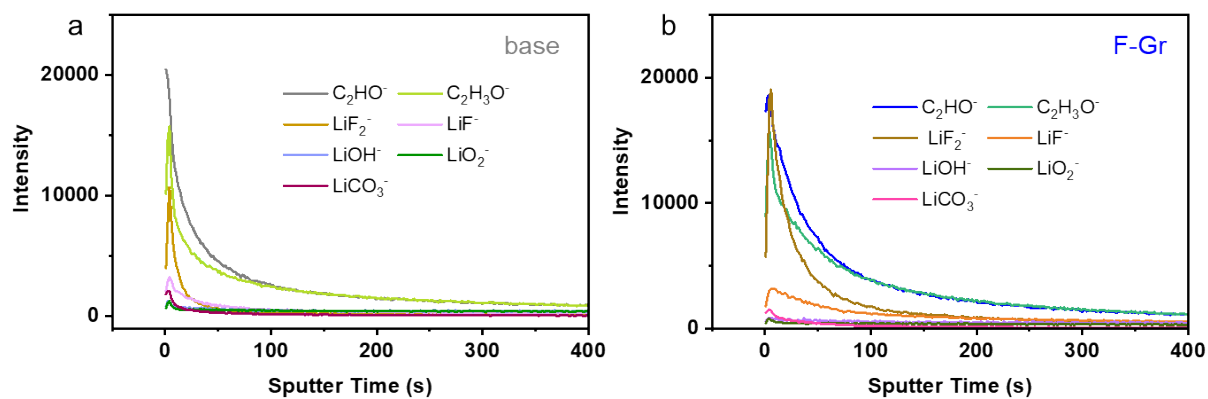
Figure S9. TOF-SIMS depth profiles with intensity of cycled Li-metal (1 mA cm^{-2}, 1 mAh cm^{-2}, 50 cycles) with (a) base electrolyte and (b) F-Gr-contained electrolyte in spectrometry negative-ion mode, respectively.
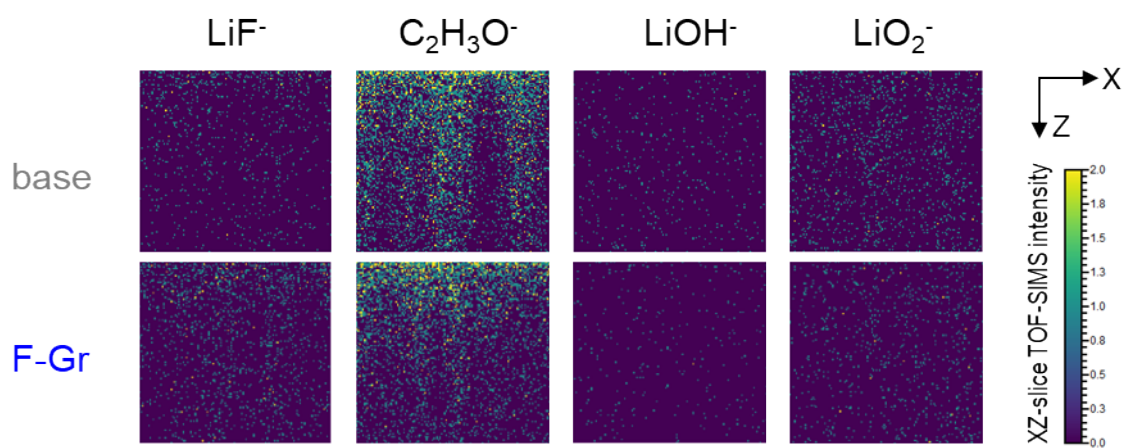
Figure S10. The intuitive 2D plane reconstructed images in XZ direction of typical ion fragments.
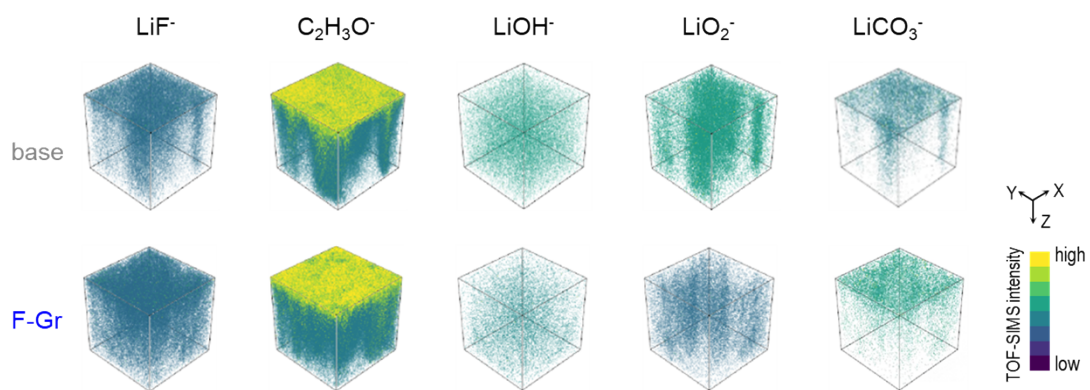
Figure S11. TOF-SIMS 3D render images of Li-metal surface after electrochemical cycling process in the base and F-Gr-contained electrolyte.
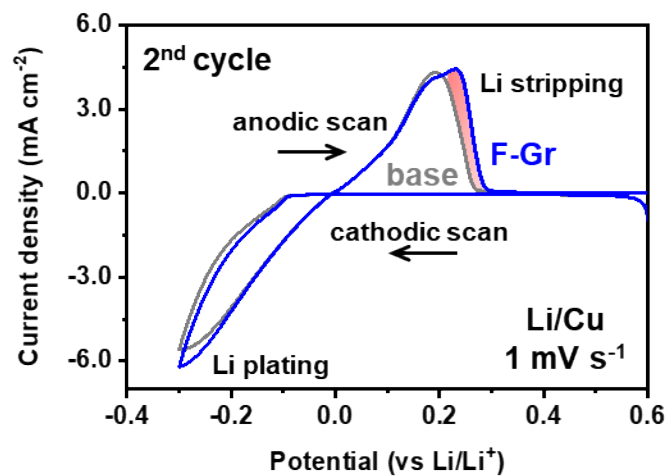
Figure S12. CV curves of Li/Cu half cells with base (gray trace) and F-Gr-contained (blue trace) electrolytes during the second cycle with a scan rate of 1 mV s^{-1}.
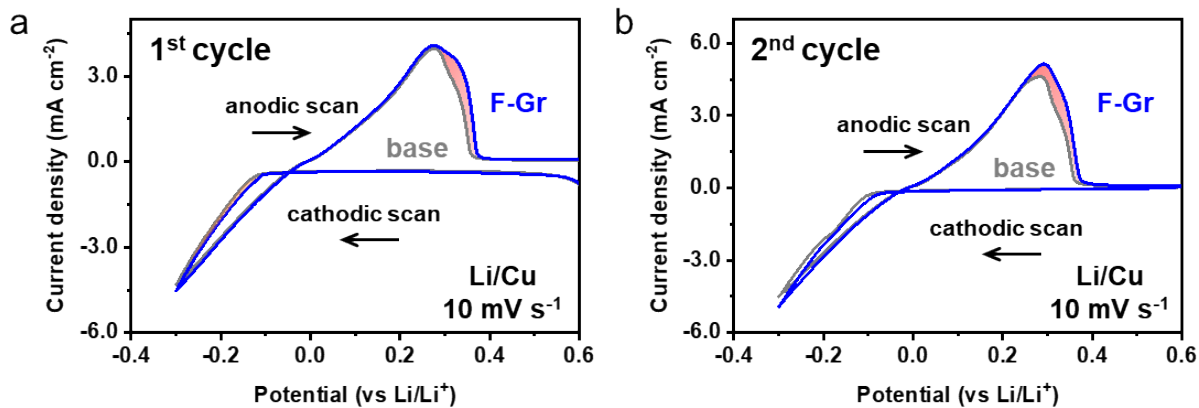
Figure S13. CV curves of Li/Cu half cells with base (gray trace) and F-Gr-contained (blue trace) electrolytes during (a) the first and (b) second cycle with a scan rate of 10 mV s^{-1}.
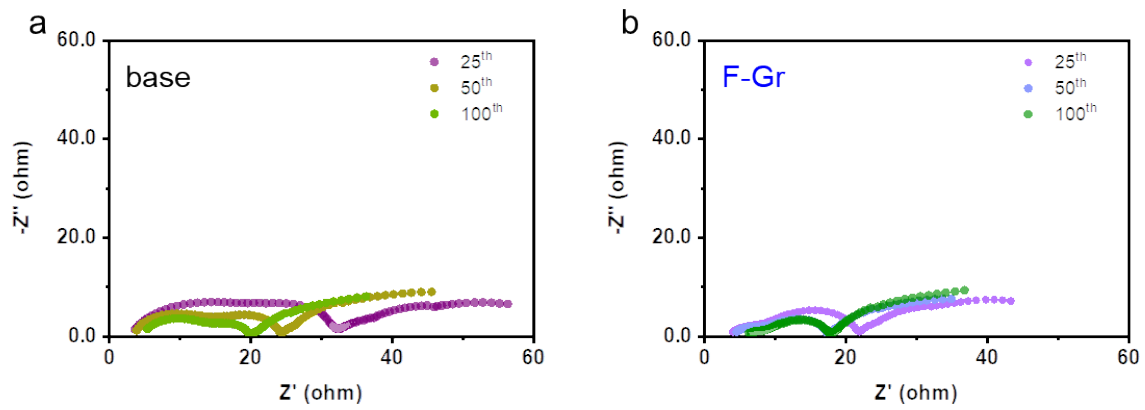
Figure S14. EIS curve in EC/EMC-based electrolyte (a) without and (b) with F-Gr for Li/Li symmetrical cells (25, 50, 100 cycles).
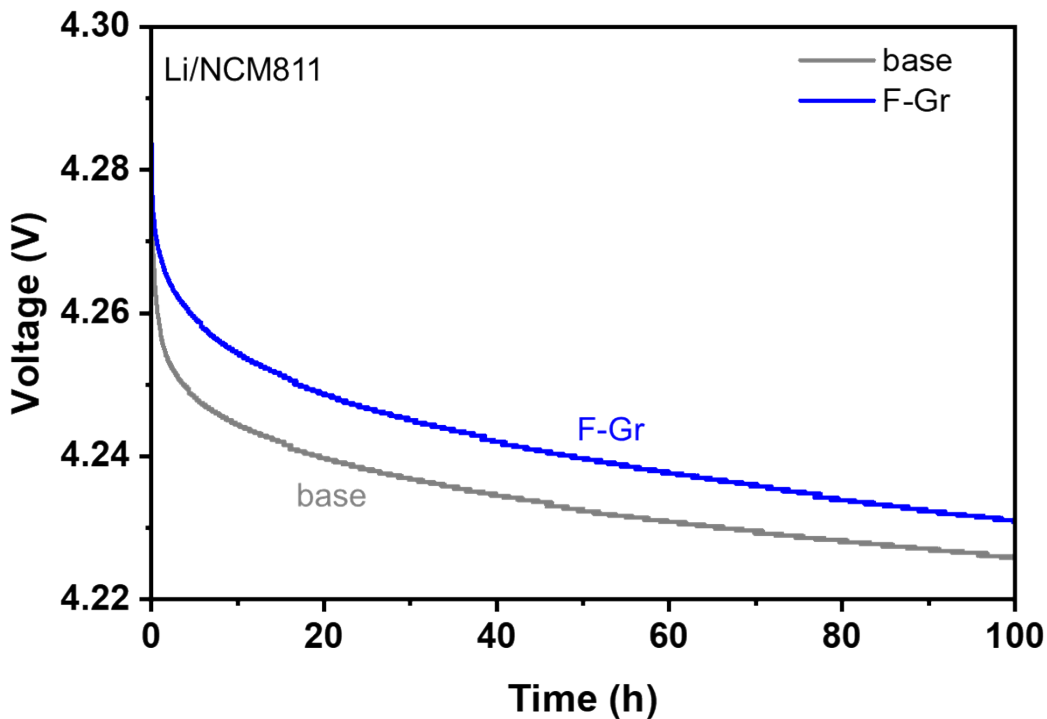
Figure S15. Voltage decay profiles of charged Li/NCM811 cells in base and F-Gr-contained electrolytes (base: gray trace, F-Gr-contained electrolyte: blue trace).

Self-discharge phenomena can be represented by the variation of the open-circuit voltage of battery under certain condition. Herein, to describe and analyze the self-discharge behavior of Li/NCM cells with base and F-Gr-contained electrolyte, the experiment to in-situ monitoring the open-circuit voltage during open circuits is conducted. After charging to 4.3 V, the open-circuit voltages of Li/NCM811 cells are monitored during resting for 100 hours. Variations in the open-circuit voltage of the charged cells are measured as a function of resting time, which are exhibited in Figure S15. In F-Gr-contained electrolyte, the descent rate of Li/NCM811 cell's voltage is significantly lower than that in base electrolyte, indicating a self-discharge suppression by F-Gr. Generally, the self-discharge behavior can be mostly ascribed to the decomposition of electrolytes in typical lithium-ion batteries. The preferential oxidation of F-Gr additive can effectively prevent

detrimental EC/EMC-based electrolyte decomposition, resulting in the distinctly suppressed self-discharge behavior of Li/NCM811 cell.

Reference:

[S1] X. Liao, Q. Huang, S. Mai, X. Wang, M. Xu, L. Xing, Y. Liao, W. Li. J. Power Sources, 2014, 272, 501-507.

[S2] P. Hong, M. Xu, B. Liao, Y. Wu, N. Lin, Q. Huang, W. Li. J. Electrochem. Soc., 2017, 164, A2914-A2921

[S3] W.-T. Xu, H.-J. Peng, J.-Q. Huang, C.-Z. Zhao, X.-B. Cheng, Q. Zhang. ChemSusChem, 2015, 8, 2892-2901

[S4] J. Sun, J. Zhang, S. Wang, P. Sun, J. Chen, Y. Du, S. Wang, I. Saadoune, Y. Wang, Y. Wei. Energy Environ. Sci., 2024, 17, 4304-43188